

Constraints of molybdenite Re–Os and scheelite Sm–Nd ages on mineralization time of the Kukaazi Pb–Zn–Cu–W deposit, Western Kunlun, NW China

Chengbiao Leng¹  · Yuhui Wang^{1,2} · Xingchun Zhang¹ · Jianfeng Gao¹ · Wei Zhang^{1,3} · Xinying Xu⁴

Received: 29 March 2017 / Revised: 3 July 2017 / Accepted: 20 July 2017 / Published online: 26 July 2017
© Science Press, Institute of Geochemistry, CAS and Springer-Verlag GmbH Germany 2017

Abstract The Kukaazi Pb–Zn–Cu–W polymetallic deposit, located in the Western Kunlun orogenic belt, is a newly discovered skarn-type deposit. Ore bodies mainly occur in the forms of lenses and veins along beddings of the Mesoproterozoic metamorphic rocks. Three ore blocks, KI, KII, and KIII, have been outlined in different parts of the Kukaazi deposit in terms of mineral assemblages. The KI ore block is mainly composed of chalcopyrite, scheelite, pyrrhotite, sphalerite, galena and minor pyrite, arsenopyrite, and molybdenite, whereas the other two ore blocks are made up of galena, sphalerite, magnetite and minor arsenopyrite and pyrite. In this study, we obtained a molybdenite isochron Re–Os age of 450.5 ± 6.4 Ma (2σ , MSWD = 0.057) and a scheelite Sm–Nd isochron age of 426 ± 59 Ma (2σ , MSWD = 0.49) for the KI ore block. They are broadly comparable to the ages of granitoid in the region. Scheelite grains from the KI ore block contain high abundances of rare earth elements (REE, 42.0–95.7 ppm) and are enriched in light REE compared to heavy REE, with negative Eu anomalies ($\delta\text{Eu} = 0.13\text{--}0.55$). They display

similar REE patterns and Sm/Nd ratios to those of the coeval granitoids in the region. Moreover, they also have similar Sr and Nd isotopes [$^{87}\text{Sr}/^{86}\text{Sr} = 0.7107\text{--}0.7118$; $\varepsilon_{\text{Nd}}(\text{t}) = -4.1$ to -4.0] to those of such granitoids, implying that the tungsten-bearing fluids in the Kukaazi deposit probably originate from the granitic magmas. Our results first defined that the Early Paleozoic granitoids could lead to economic Mo–W–(Cu) mineralization at some favorable districts in the Western Kunlun orogenic belt and could be prospecting exploration targets.

Keywords Molybdenite Re–Os · Scheelite Sm–Nd · REE · Kukaazi Pb–Zn–Cu–W polymetallic deposit · Western Kunlun orogenic belt

1 Introduction

Timing of mineralization is very important for understanding and interpreting metallogenesis and is thus useful for establishing the metallogenetic model. Direct isotopic dating of suitable minerals has been proved as a possible approach to resolving the age of ore formation (Chesley et al. 1991). Due to high rhenium (Re) and very low common osmium (Os) concentrations, Re–Os dating of molybdenite has become a powerful tool to constrain the ages of mineralization directly (Stein et al. 1997). Scheelite, a common accessory mineral in many hydrothermal deposits with high contents of REE, Sr, and Pb and variable Sm/Nd ratios (e.g., Bell et al. 1989; Voicu et al. 2000; Brugger et al. 2002), has also been used to constrain timing of mineralization and to trace the source(s) of ore-forming fluids for hydrothermal deposits, especially for hydrothermal W–Au deposits (e.g., Frei et al. 1998; Peng et al. 2003, 2006).

✉ Chengbiao Leng
lengchengbiao@vip.gyig.ac.cn

Xingchun Zhang
zhangxingchun@vip.gyig.ac.cn

¹ State Key Laboratory of Ore Deposit Geochemistry, Institute of Geochemistry, Chinese Academy of Sciences, Guiyang 550081, China

² Guizhou Central Laboratory of Geology and Mineral Resources, Guiyang 550018, China

³ University of Chinese Academy of Sciences, Beijing 100049, China

⁴ Tianjin Institute of Geology and Mineral Resources, Tianjin 300170, China

The Kukaazi Pb–Zn–Cu–W polymetallic deposit is currently discovered in the metamorphic rocks of the Mesoproterozoic Changcheng Group in the Western Kunlun orogenic belt (WKOB). In this deposit and its adjacent regions, a number of Ordovician granodiorite and monzonite intrusions (471–441 Ma; Wang et al. 2013a, b; Zhang et al. 2015) were emplaced into the Changcheng Group. However, due to a lack of mineralization age and isotopic data for the Kukaazi deposit, the genetic relationship between the mineralization and such Ordovician granitoid magmatism remains unclear, which limited the understanding of metallogenesis of the region. Here we present molybdenite Re–Os and scheelite Sm–Nd isochron ages to constrain the timing of Mo and W mineralization at the Kukaazi deposit. In addition, REE contents, Sr, and Nd isotopes of the scheelite are also provided to constrain the sources of ore-forming fluids and metals.

2 Geological setting

The Kukaazi deposit, with coordinates of 76°39.5' E, 37°10' N at its center, is located in the WKOB, which is an over 2000 km long NW–SE-trending narrow structural belt between the Tarim Craton and the Karakorum–Qiangtang Block (Fig. 1a; e.g., Xu et al. 2011; Zhang et al. 2015). Previous researches indicated that the WKOB can be divided into the North Kunlun Terrane (NKT), the South Kunlun Terrane (SKT), and the Taxkorgan-Tianshuihai Terrane (TST) (Fig. 1b). They are bordered by the Akazi-Kegang Fault and the Mazha-Kangxiwa Fault from north to south, respectively (e.g., Pan 1989; Mattern et al. 1996; Mattern and Schneider 2000; Xiao et al. 2002; Zhang et al. 2015). The NKT, bounded by the Tiekelike Fault to the north and the Akazi-Kegang Fault to the south, was generally considered to be a part of the Tarim Craton in the Paleo-Proterozoic (Pan et al. 1994; Xu et al. 1994; Jiang et al. 2000; Yuan et al. 2003). It is mainly composed of the Proterozoic to Lower Paleozoic metamorphic rocks, which are overlain by the Devonian to Triassic carbonate and clastic rocks locally (Xiao et al. 2002). Previous studies confirmed that the metamorphic basement of the NKT was probably formed during 2.4–0.8 Ga (Zhang et al. 2004, 2007; Wang et al. 2009). The SKT is sandwiched between the Akazi-Kegang and Mazha-Kangxiwa faults. It is characterized by the existence of Precambrian gneiss-schist-migmatite complex and the Kudi ophiolite (Yin and Harrison 2000; Xiao et al. 2002), and its southern part is occupied by many Early Carboniferous to Late Triassic arc-type magmatic rocks (Xiao et al. 2002). According to Yuan et al. (2002), the Precambrian metamorphic rocks of the SKT have much younger depleted mantle Nd model ages (i.e. 1.5–1.1 Ga) than those of the North Kunlun Terrane

(>2.8 Ga). Meanwhile, the timing of the Kudi ophiolite suite was constrained between 525 and 510 Ma through high-precision SHRIMP zircon U–Pb dating by some researchers (e.g., Xiao et al. 2003; Zhang et al. 2004). In the TST, there are outcropping a series of Permo-Triassic flysch-facies sedimentary rocks, similar to those of the Bayan Har Block in terms of lithological assemblages (Mattern et al. 1996). The TST has been considered to be a giant accretionary wedge formed by the northward subduction of the Paleo-Tethyan ocean basin (Xiao et al. 2005).

From Early Paleozoic to Triassic, the WKOB had experienced the Proto-Tethyan to the Paleo-Tethyan oceans evolutions (Pan et al. 1994; Mattern et al. 1996; Mattern and Schneider 2000; Xiao et al. 2002, 2005; Xu et al. 2015; Zhang et al. 2015). With the expansion, subduction, and closure of the different stages of Tethyan oceanic basins, a large amount of granitoids were emplaced into the western Kunlun area along the striking orientation of the orogenic belt and were controlled by the regional fracture zones (Fig. 1b) (Wang et al. 2013a; Zhang et al. 2015). The Early Paleozoic granite intrusions are distributed mainly in the South Kunlun and North Kunlun terranes, and intruded the metamorphic basement rocks during 521–431 Ma (Fig. 1b; Zhang and Xie 1989; Fang and Wang 1990; Xu et al. 1994; Jiang et al. 1999, 2000; Yuan et al. 2003; Cui et al. 2006, 2007; Yu et al. 2011; Wang et al. 2013a). These granites exhibit arc signatures (i.e. negative anomalies of Nd, Ta, and Ti) and are suggested to originate from partial melting of mafic lower crust in an active continental arc setting (Yuan et al. 2003; Wang et al. 2013a; Jia 2013). The Early Mesozoic granitoids (243–192 Ma) are mainly distributed along the line of the Mazha-Kangxiwa Fault (Fig. 1b; Zhang et al. 2005, 2015). They comprise metaluminous I-type granodiorite and monzogranite and have geochemical features similar to the bulk continental crust, which was ascribed to be resulted from melting of amphibolite of mid-ocean-ridge basalt protolith during continental collision stages (Zhang et al. 2015).

The WKOB is an important Cu–Pb–Zn–Au mineral deposit belt in China (Sun et al. 2003; Zhang et al. 2014c) and is also a famous place for producing high-quality nephrite (usually called Hetian nephrite) for the world (Liu et al. 2016). Four kinds of metallic ore deposits have been discovered in the WKOB (Fig. 1b). They include (1) carbonate-hosted Cu–Pb–Zn–(Au–Co) deposits (e.g., the Tiekelike Cu–Pb–Zn–Ag, Tamu Zn–Pb–Co, Kalangu Pb–Zn–Co, and Bulunkou Cu–Au deposits; Sun et al. 2003; Zhang et al. 2014c), (2) volcanic-hosted massive sulfide Cu–(Zn) deposits (e.g., the Saluoyi Cu, Aketashi Cu, and Shangqihan Cu–Zn deposits; Sun et al. 2003), (3) magmatic-hydrothermal Cu–Mo–Fe–(Li–Be) deposits (e.g., the Datong porphyry Cu–Mo, Kayizi porphyry Mo, Kudi skarn Cu–Fe,

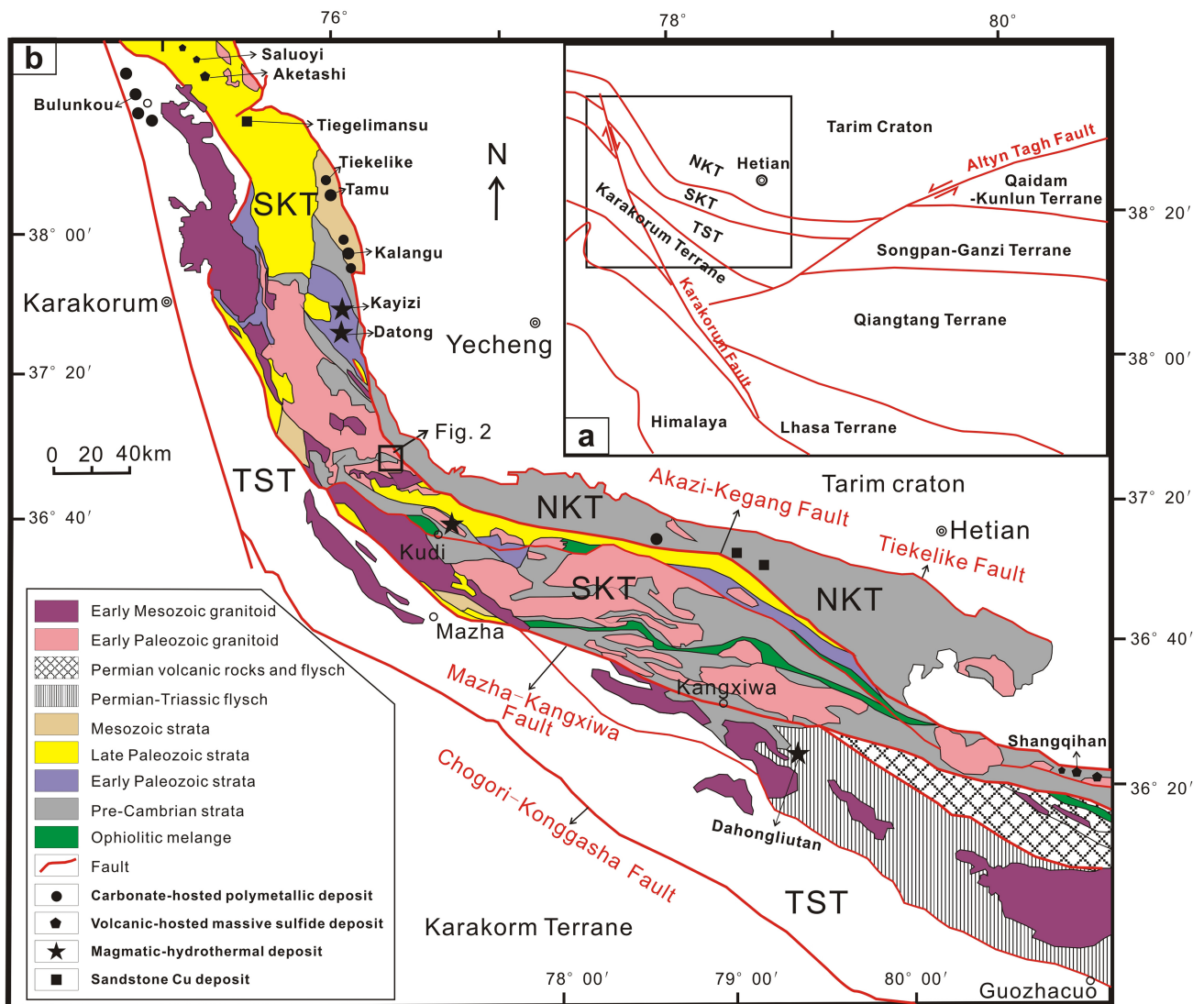


Fig. 1 **a** A schematic map of the Western Kunlun orogenic belt and its adjacent regions (modified after Zhang et al. 2015), and **b** a simplified geologic map of the Western Kunlun orogenic belt (modified from Wang et al. 2013a and Zhang et al. 2015). In **b**, NKT North Kunlun Terrane, SKT South Kunlun Terrane, TST Taxkorgan-Tianshuihai Terrane; and some represented metallic ore deposits are also labeled

and Dahongliutan Li–Be deposits; Sun et al. 2003; Liu et al. 2010), and (4) sandstone Cu deposits (e.g., the Tegelimansu Cu deposit; Sun et al. 2003). The carbonate-hosted Cu–Pb–Zn deposits formed in two epochs, 337–331 and 235–206 Ma (Zhang et al. 2014c). The VMS Cu–(Zn) deposits are hosted in the Carboniferous bimodal volcanic rocks with a whole-rock Rb–Sr isochron age of 332 ± 66 Ma (Sun et al. 2003). While these magmatic-hydrothermal Cu–Mo–Fe–(Li–Be) deposits are closely associated with some felsic intrusions. According to Liu et al. (2010), the molybdenite Re–Os ages of the Kayizi porphyry deposit is consistent with the zircon U–Pb age (251 ± 5) of the ore-bearing granitoids therein. The Tegelimansu sandstone Cu deposit is hosted in the Early Carboniferous red clastic rocks (Sun et al. 2003). Therefore, both the geologic

evidence and the available isotopic data suggest that the aforementioned four types of metallic ore deposits were formed in the Late Paleozoic. However, the linkage between the mineralization and the Early Paleozoic granitic intrusions is still unclear, although such granitoids are extensively distributed in the western Kunlun.

3 Geology of the Kukaazi deposit

3.1 Wall rocks

Outcropped strata in the Kukaazi mine are mainly composed of the low-grade metamorphosed clastic rocks, meta-volcanic rocks, marble, and minor garnet skarns of

the Middle Proterozoic Changcheng Group (Fig. 2a), with a strike of 160° – 210° and a steep dip angle of 60° – 80° (Fig. 2b). The Ordovician granitic plutons, including monzonite, granodiorite, and minor K-feldspar granite, were emplaced into the metamorphic rocks during 462–456 Ma in the deposit (Wang et al. 2013b). These plutons belong to metaluminous I-type granites, with A/CNK values between 0.91 and 1.05. They are enriched in light REE and large ion lithophile elements, relatively depleted in high field strength elements (i.e. Nb, Ta, Ti, P), and possess high initial Sr isotopic ratios and negative $\varepsilon_{\text{Hf}}(\text{t})$ values (Yuan et al. 2003; Wang et al. 2013a; Jia 2013). Hence, they were proposed to result from partial melting of the mafic lower crust of the SKT in an active continental arc setting (Yuan et al. 2003; Wang et al. 2013a, b).

3.2 Ore bodies

Ore bodies of the Kukaazi deposit mainly occur in the forms of lenses and veins along beddings of various low-grade metamorphic rocks of the Mesoproterozoic Changcheng Group, which is composed of marble, mica quartz slate, meta-volcanic rocks, and chlorite slate. According to mineral assemblage and spatial distribution, three ore blocks (KI, KII, and KIII) have been outlined in the mine (Fig. 2a).

The KI ore block occurs at the northwest of the mine and is composed of chalcopyrite, scheelite, sphalerite, galena, plus minor pyrite, pyrrhotite, arsenopyrite,

molybdenite, tetrahedrite, and bismuthinite (Fig. 3). The ores mainly occur in four layers of garnet skarns between a hanging wall of laminated marble and a footwall of the siliceous meta-tuffaceous rocks (Fig. 2b). The garnet skarn ore is composed of irregular garnet and marble, with quartz, sulfides, and scheelite grains occurring as patchy aggregates and veins. Marble ore, containing sphalerite, galena, arsenopyrite, and pyrite, is distributed along beddings of the Changcheng Group (Fig. 2b). The ore bodies are overall 80–200 m long and 3–12 m wide. A large Cu–W–(Zn–Pb) ore body is over 6 meters in thickness, with average grades of 0.9 wt% for Cu, 0.2 wt% for WO_3 (up to 0.92 wt%), 0.8 wt% for Zn, and 0.3 wt% for Pb, respectively. The gangue minerals mainly include garnet, quartz, carbonate, and minor fluorite.

The KII ore block is located at the center of the mine. In this ore block, three lens-shaped massive ore bodies (comprising of galena + sphalerite + magnetite + pyrite \pm pyrrhotite \pm chalcopyrite) occur within coarse-grained crystalline marble or between the beddings of marble and tuffaceous slate. The ore bodies are 5–10 m thick (up to 14 m), 80 m long, with average ore grades of 13.7 wt% for Pb and 9.9 wt% for Zn.

The KIII ore block is sited at the southeast of the mine. The lens-shaped ore bodies, consisting of galena + sphalerite + magnetite \pm arsenopyrite \pm pyrite \pm bismuthinite, are hosted in garnet-diopside skarns along the beddings of the marble and meta-rhyolitic tuff or quartz keratophyre.

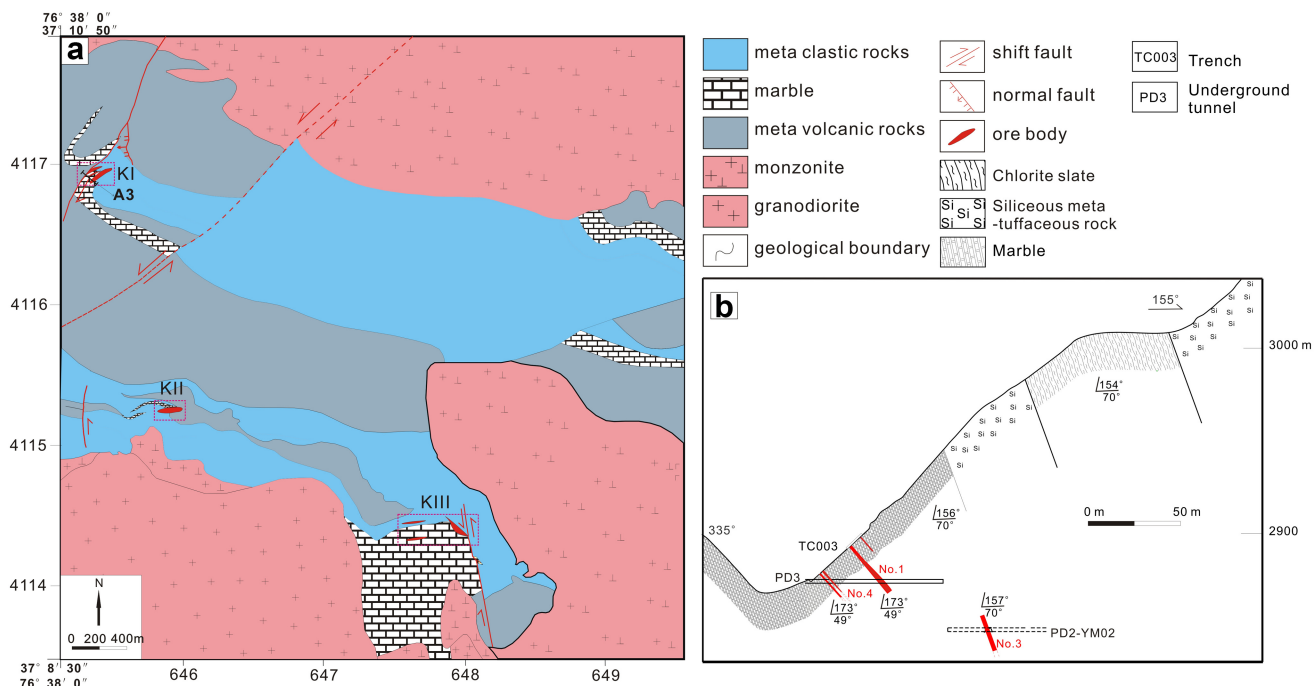


Fig. 2 **a** A simplified regional geological map of the Kukaazi deposit, and **b** a geological cross section along exploration line A3 (its location labeled in **a**)

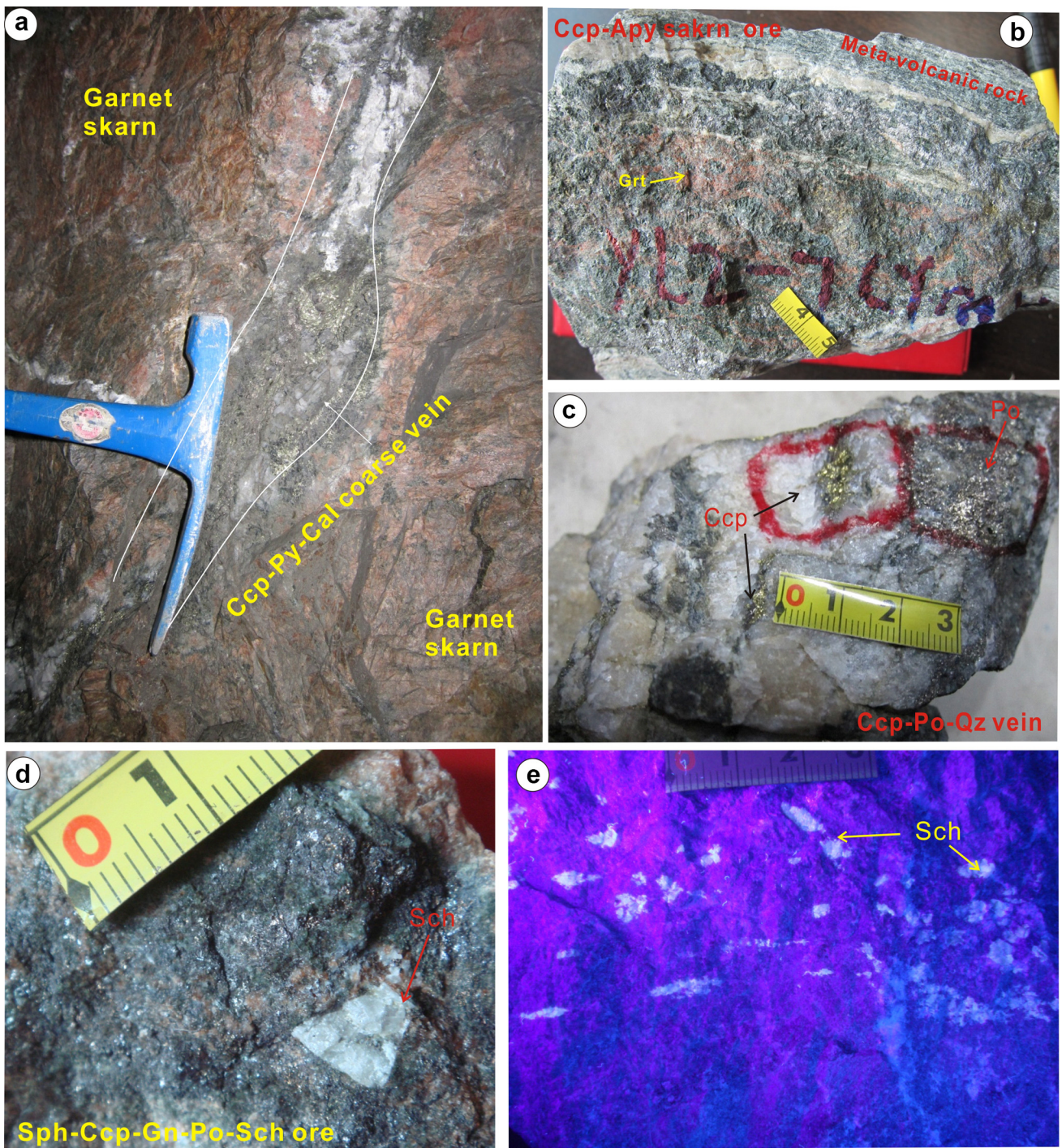


Fig. 3 Photographs of some representative ores from the Kukaazi deposit: **a** a chalcopyrite–pyrite–calcite coarse vein in the garnet skarn; **b** a specimen of chalcopyrite–arsenopyrite skarn ore; **c** a chalcopyrite–pyrrhotite–quartz vein; **d** a scheelite grain in sphalerite–galena–chalcopyrite–pyrrhotite–arsenopyrite ore specimen; **e** scheelite in ores under ultraviolet light. Mineral abbreviations: *Apy* arsenopyrite, *Cal* calcite, *Ccp* chalcopyrite, *Gn* galena, *Grt* garnet, *Po* pyrrhotite, *Py* pyrite; *Qz* quartz; *Sch* scheelite; *Sph* sphalerite

3.3 Paragenesis of the mineralization

Two stages of mineralization, including the early diagenesis stage and the late magmatic-hydrothermal stage, have

been identified at the Kukaazi deposit (Zhang et al. 2014b). The oolitic pyrite, tiny grains of Fe-rich sphalerite, galena, and pyrrhotite in massive sulfide ores in marble were formed in the diagenetic process. The association of

chalcopyrite, scheelite, molybdenite, and coarse-grained pyrrhotite, sphalerite, galena, and arsenopyrite in veins suggests that they were formed from magmatic-hydrothermal fluids. Based on field and microscopic observations of cross-cutting relationships and textures of various minerals, we draw the mineral paragenesis diagram for the Kukaazi deposit (Fig. 4).

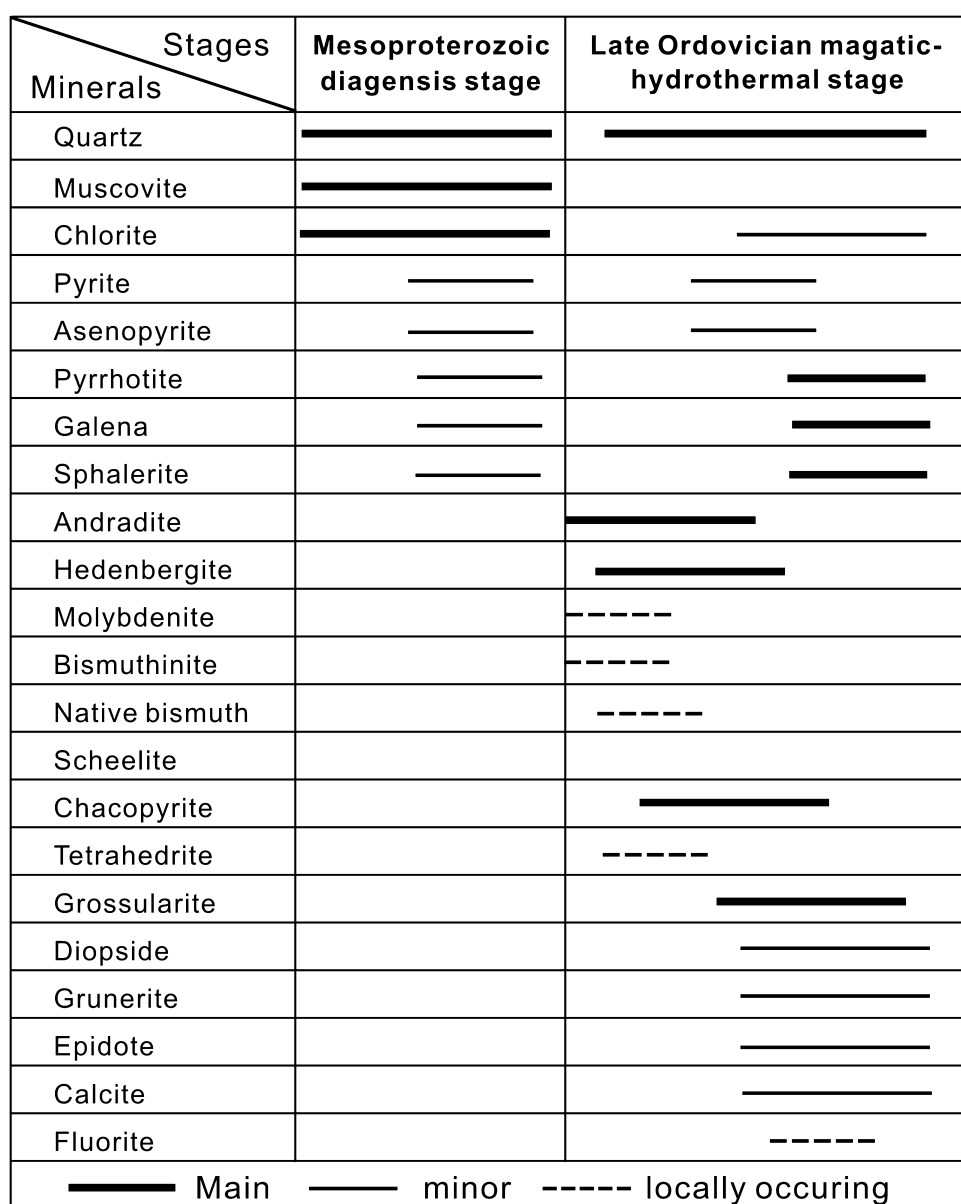
4 Analytical methods

4.1 Molybdenite Re–Os analytical methods

Four molybdenite samples were selected from the KI ore block to undertake Re–Os isotopic dating. Froth flotation

was first applied to separate molybdenite from the finely crushed mineralized rocks. Then molybdenite separates were handpicked individually under a binocular microscope to get over 99% purity. Re–Os isotope analysis was performed on a Thermo ICP-MS (X7) in the Re–Os Laboratory, National Research Center of Geoanalysis, Chinese Academy of Geological Sciences in Beijing. The detailed analytical procedures are described in Du et al. (1994, 2004). A model age of 220.6 ± 3.2 Ma, which is consistent with the certified value of 221.4 ± 5.6 Ma (Du et al. 2004), for the molybdenite standard GBW04435 (HLP) has been obtained in this analysis. Procedure blanks were 1.3 ± 0.2 pg for Re and 0.21 ± 0.06 pg for Os, respectively. The ^{187}Re decay constant of 1.666×10^{-11}

Fig. 4 Simplified paragenetic sequence of ore and gangue minerals for the Kukaazi deposit



year⁻¹ (Smolar et al. 1996) was used to calculate the molybdenite model ages.

4.2 Sm–Nd, and Sr isotopes analyses of the scheelite

Nine scheelite-bearing ore samples were also collected from KI ore block to obtain scheelite separates. Sm–Nd and Sr isotopes of scheelite were analyzed at the Tianjin Institute of Geology and Mineral Resources (TIGMR). 0.15 g sample powder was weighted and dissolved by HF + HClO₄ solution in sealed Teflon reaction container at high temperature for half a day. The Sr obtained through Isotope Concentration procedure needed to be doubly purified. The phosphoric acid (HDEHP) method was applied for the Nd purification. Measurement of Sm–Nd–Sr isotopic compositions was carried out on a Triton thermal ionization mass spectrometer (TIMS). Sr and Nd isotopic ratios were normalized to ⁸⁸Sr/⁸⁶Sr ratio of 8.37521 and for ¹⁴⁶Nd/¹⁴⁴Nd ratio of 0.7219, respectively. The measured results were 0.710253 ± 6 for ⁸⁷Sr/⁸⁶Sr ratio of the Standard NBS987 and 0.511132 ± 5 for ¹⁴³Nd/¹⁴⁴Nd ratio of the Standard JMC, respectively, with standard deviation of 2σ. The measured results of the Standard NBS-607 (K-feldspar) were 522 ppm for Rb, 65.3 ppm for Sr, and 1.200050 ± 5 for ⁸⁷Sr/⁸⁶Sr ratio. The measured results of the China First Class Standard GBS04419 (rock) were 3.02 ppm for Sm, 10.07 ppm for Nd, and 0.512739 ± 5 for ¹⁴³Nd/¹⁴⁴Nd ratio. The measured results of the International Standard BCR-2 (basalt) were 6.61 ppm for Sm, 28.13 ppm for Nd, and 0.512643 ± 5 for ¹⁴³Nd/¹⁴⁴Nd ratio. The blank of the whole procedure was 56 ng for Rb, 38 ng for Sr, 30 pg for Sm, and 54 pg for Nd, respectively. The Sm–Nd isochron age was calculated by using Isoplot/Exversion 4.15 (Ludwig 2012).

4.3 REE analysis of the scheelite

REE analyses of thirteen scheelite samples were conducted at the State Key Laboratory of Ore Deposit Geochemistry (SKLODG), Institute of Geochemistry Chinese Academy of Sciences using PE Elan DRC-e inductively coupled plasma-mass spectrometry (ICP-MS) and with analytical precision and accuracy generally better than 10%. The detailed analytical procedures were broadly similar to those described in Qi et al. (2000).

5 Results

5.1 Re–Os ages of molybdenite

Rhenium, Os concentrations and isotopic ratios of the molybdenite are listed in Table 1. Total Re and ¹⁸⁷Os

concentrations vary from 47.7 to 134 ppm and from 226 to 635 ppb, respectively. All the Re–Os model ages are in a narrow variation, from 451.9 ± 6.3 to 450.5 ± 7.1 Ma. They show an excellent reproducibility, and yield an ¹⁸⁷Re–¹⁸⁷Os isochron age of 450.5 ± 6.4 Ma (2σ, MSWD = 0.057, N = 4), with a weighted average age of 451.3 ± 3.4 Ma (2σ, MSWD = 0.037, N = 4) (Fig. 5). The intercept on the ¹⁸⁷Os axis is nearly zero within uncertainty, which indicates that the isochron age of the molybdenite is reliable.

5.2 Sm–Nd and Sr isotopic compositions of scheelite

¹⁴⁷Sm/¹⁴⁴Nd and ¹⁴³Nd/¹⁴⁴Nd ratios of the scheelite range from 0.0879 to 0.1176 and from 0.512128 to 0.512211, respectively (Table 2). They yield an isochron age of 426 ± 59 Ma (2σ, MSWD = 0.49, N = 9), with an initial ¹⁴³Nd/¹⁴⁴Nd ratio of 0.511882 ± 0.000038 (Fig. 6a). Since this age is consistent with the molybdenite Re–Os age within uncertainty, and no linear relationship between the (¹⁴³Nd/¹⁴⁴Nd)_t and 1/Nd ratios (Fig. 6b), it is thus believed that this Sm–Nd isochron age of the scheelite is acceptable. Taking 426 Ma as the tungsten mineralization time, the calculated initial ¹⁴³Nd/¹⁴⁴Nd values vary from 0.511879 to 0.511884 (average 0.511882) (Table 2), with uniform ε_{Nd(t)} values of ca. -4.0. Their depleted mantle Nd model ages (T_{DM}) vary from 1.5 to 1.2 Ga (average 1.3 Ga), consistent with the model ages of the coeval granitoids in the area (Yuan et al. 2003; Jia 2013).

The scheelite has uniform Sr isotopic compositions, with ⁸⁷Sr/⁸⁶Sr varying from 0.7107 to 0.7118.

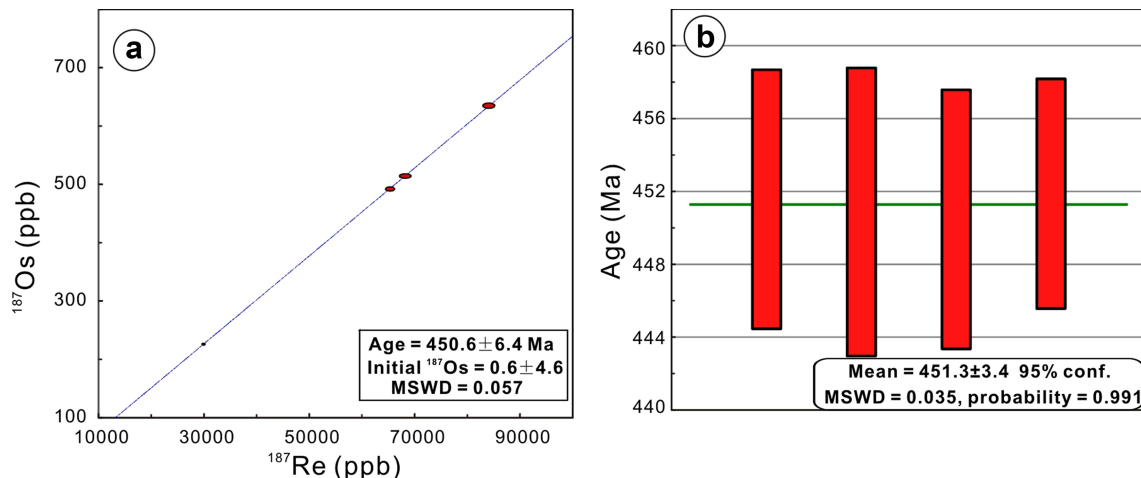
5.3 REE compositions

REE concentrations and calculated parameters of the scheelite are given in Table 3. The Sm and Nd contents are broadly consistent with those measured by isotope dilution method within the ranges of standard deviation (Table 2). This means that these analytical results were reliable. The scheelite has high contents of REE (including Y, 42–96 ppm), similar to the scheelite from the Woxi Au–Sb–W deposit (41–124 ppm, Peng et al. 2005) but much lower than the scheelite from the Daping Au (1760–2004 ppm, Xiong et al. 2006) and Xuebaoding W–Sn–Be deposits (369–1302 ppm, Liu et al. 2007) in China.

The scheelite is characterized by strong enrichments of light REE (LREE) compared to heavy REE (HREE), with the La/Yb_N ratios varying from 33 to 226 (Table 3; Fig. 7). These REE features are similar to those of scheelite from the porphyry and skarn types deposits (Fig. 8; Song et al. 2014) but are obviously contrasted to the scheelite from the

Table 1 Re-Os data for molybdenite from the Kukaazi deposit

Sample	Weight (g)	Re (ppm)		^{187}Re (ppm)		^{187}Os (ppb)		Model age (Ma)	
		Measured	$\pm 2\sigma$	Measured	$\pm 2\sigma$	Measured	$\pm 2\sigma$	Measured	$\pm 2\sigma$
YL-4	0.01042	133.9	1.5	84.13	0.92	635.4	3.6	451.6	7.1
YL-13-11	0.00539	108.6	1.4	68.27	0.90	514.8	3.1	450.9	7.9
YL-13-12	0.00403	104.0	1.1	65.38	0.70	492.5	3.0	450.5	7.1
YL-47-2	0.00533	47.65	0.37	29.95	0.24	226.3	1.3	451.9	6.3

**Fig. 5** **a** A Re–Os isochron age diagram, and **b** a Re–Os weighted average model age diagram for molybdenite samples from the Kukaazi deposit**Table 2** Sm, Nd, and Sr isotopic compositions of the scheelite from the Kukaazi deposit

Sample	$^{87}\text{Sr}/^{86}\text{Sr}$ (2σ)	Sm (ppm)	Nd (ppm)	$^{147}\text{Sm}/^{144}\text{Nd}$	$^{143}\text{Nd}/^{144}\text{Nd}$ (2σ)	$^{143}\text{Nd}/^{144}\text{Nd}$ ($t = 426$ Ma)	ε_{Nd} ($t = 426$ Ma)	T _{DM} (Ga)
BWK-1	0.710916 (13)	2.934	17.39	0.1020	0.512168 (3)	0.511884	-4.0	1.3
BWK-3	0.710905 (9)	1.938	13.33	0.0879	0.512128 (7)	0.511883	-4.0	1.2
BWK-4	0.711111 (15)	3.712	23.20	0.0967	0.512153 (5)	0.511883	-4.0	1.3
BWK-6	0.710785 (10)	3.295	16.94	0.1176	0.512211 (12)	0.511883	-4.0	1.5
BWK-13	0.710718 (8)	2.669	15.51	0.1040	0.512169 (7)	0.511879	-4.1	1.4
BWK-15	0.710875 (3)	2.670	16.70	0.0966	0.512149 (5)	0.511880	-4.1	1.3
BWK-16	0.710902 (5)	3.276	19.90	0.0995	0.512156 (7)	0.511879	-4.1	1.3
BWK-18	0.711847 (6)	3.734	22.10	0.1022	0.512168 (6)	0.511883	-4.0	1.3
N-4	0.710670 (3)	1.876	12.16	0.0932	0.512144 (9)	0.511884	-4.0	1.3

lode Au–W (–Sb) deposits in South China that is characterized by middle REE- and HREE- enrichment, but LREE- depletion (Peng et al. 2005). In addition, the scheelite has remarkable negative Eu anomalies ($\delta\text{Eu} = 0.13\text{--}0.55$, average 0.36) similar to that of the scheelite from the Xuebaoding W–Sn–Be deposit ($\delta\text{Eu} = 0.44\text{--}0.51$, Liu et al. 2007) but different from that from the lode Au–W (–Sb) ore deposits with positive Eu anomalies (Peng et al. 2005).

6 Discussion

6.1 Timing of Mo and W mineralization and its geological significances

In this study, we obtained a precise molybdenite isochron Re–Os age of 450.5 ± 6.4 Ma and a rough scheelite Sm–Nd isochron age of 426 ± 59 Ma for the Kukaazi deposit. The Sm–Nd isochron age of scheelite is consistent with the

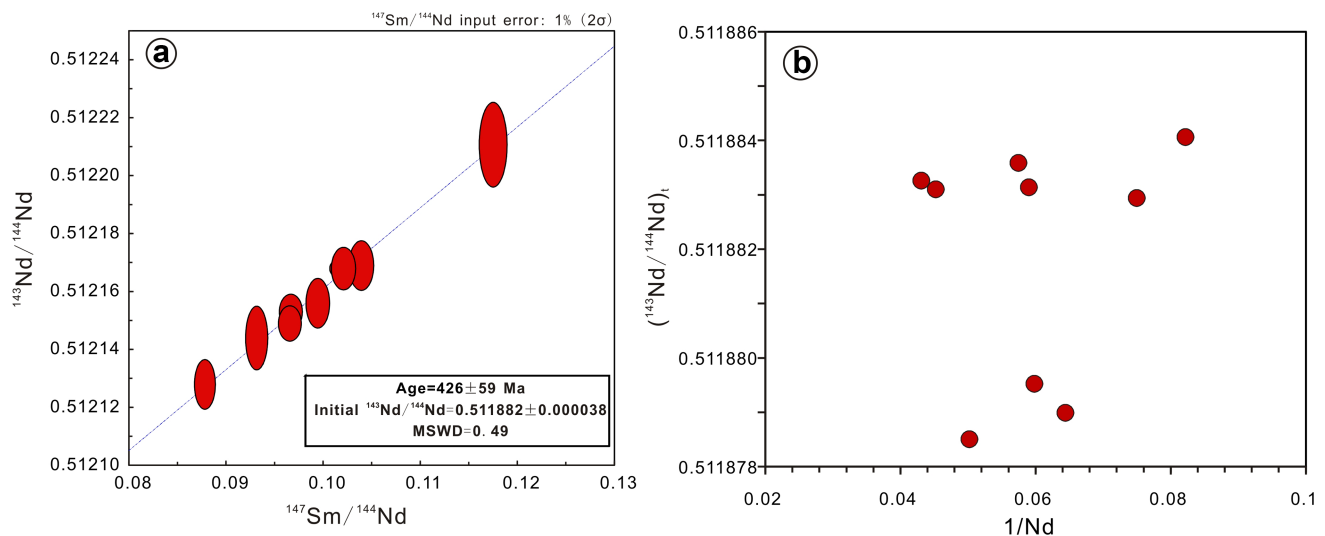


Fig. 6 **a** A Sm–Nd isochron age diagram, and **b** a plot showing $(^{143}\text{Nd}/^{144}\text{Nd})_t$ versus $1/\text{Nd}$ ratios for scheelite samples from the Kukaazi deposit

Table 3 REE concentrations (ppm) and related parameters of the scheelite from the Kukaazi deposit

Sample	BWK-1	BWK-3	BWK-4	BWK-6	BWK-7	BWK-13	BWK-15	BWK-16	BWK-18	N-2	N-3	N-4	N-7
La	9.50	8.78	10.4	10.1	15.4	9.84	12.9	10.8	15.9	5.55	13.4	7.79	21.5
Ce	21.6	17.6	28.7	25.6	36.7	24.1	30.8	28.1	29.7	17.0	30.4	18.1	35.1
Pr	2.94	2.26	4.48	3.69	5.17	3.39	4.04	4.05	3.91	2.89	4.10	2.48	4.62
Nd	11.6	9.51	19.7	15.3	20.4	12.8	15.4	17.4	16.1	14.9	16.7	10.8	20.1
Sm	2.11	1.49	3.27	2.93	2.23	2.24	2.51	2.97	2.69	3.13	2.21	1.63	3.60
Eu	0.24	0.16	0.10	0.25	0.12	0.24	0.19	0.31	0.19	0.12	0.20	0.15	0.12
Gd	1.12	0.57	1.20	1.25	0.95	0.80	0.87	1.37	1.52	2.05	0.82	0.59	2.21
Tb	0.16	0.12	0.21	0.19	0.22	0.14	0.14	0.22	0.24	0.33	0.13	0.11	0.41
Dy	0.41	0.27	0.50	0.45	0.37	0.28	0.39	0.59	0.96	1.33	0.24	0.33	1.42
Ho	0.07	0.03	0.07	0.06	0.05	0.04	0.06	0.09	0.18	0.21	0.03	0.02	0.26
Er	0.18	0.10	0.24	0.24	0.21	0.12	0.13	0.29	0.39	0.50	0.14	0.13	0.62
Tm	0.02	0.01	0.01	0.01	0.01	0.01	0.01	0.02	0.03	0.02	0.01	0.01	0.04
Yb	0.11	0.06	0.06	0.04	0.07	0.05	0.07	0.18	0.16	0.11	0.04	0.04	0.24
Lu	0.01	0.01	0.01	0.01	0.01	0.01	0.01	0.02	0.01	0.02	0.01	b.d.	0.02
Y	1.50	0.99	1.45	1.51	1.30	0.96	1.55	2.24	3.29	3.40	0.78	1.03	5.44
Total	51.6	41.89	70.45	61.71	83.3	54.96	69.05	68.64	75.39	51.60	69.28	43.2	95.74
La/Yb _N	58.7	98.1	118	158	153	147	119	39.7	67.8	32.9	226	140	61.5
δEu	0.48	0.53	0.16	0.40	0.24	0.55	0.39	0.47	0.28	0.15	0.46	0.46	0.13

b.d means below detection limits, data of Chondrite are from Boynton (1984)

Re–Os age of molybdenite within uncertainties. There is no linear relationship between the $(^{143}\text{Nd}/^{144}\text{Nd})_t$ and $1/\text{Nd}$ values (Fig. 6b), suggesting that the Sm–Nd system has not been disturbed by later geological processes such that this Sm–Nd isochron age is acceptable. Moreover, tungsten generally shares similar geochemical behaviors to Mo in magmatic-hydrothermal systems (e.g., Robb 2005). Thus, W-bearing minerals (such as scheelite) would precipitate simultaneously with molybdenite from the ore-forming

fluids, which was also the case at the Kukaazi deposit. For that reason, we proposed that the timing of Mo and W mineralization of the Kukaazi deposit took place at ~ 450 Ma.

Zircon U–Pb ages of 462–456 Ma for the monzonite and granodiorite in the Kukaazi deposit (Wang et al. 2013b) are consistent with the ages of the granites around the 128 milestone of the Route 219 (471–458 Ma, Xu et al. 1994; Yuan et al. 2003), but a little bit older than the

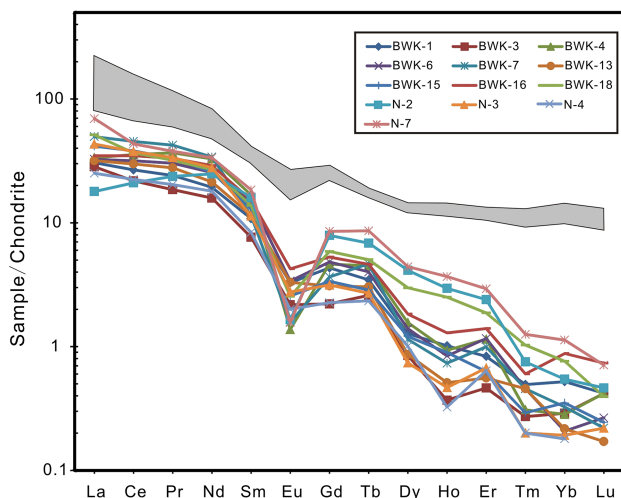


Fig. 7 Chondrite-normalized REE distribution patterns of the scheelite from the Kukaazi deposit (data of chondrite are from Boynton 1984), data of the granitoids (grey area, Wang et al. 2013b) in the deposit are also plotted here for comparison

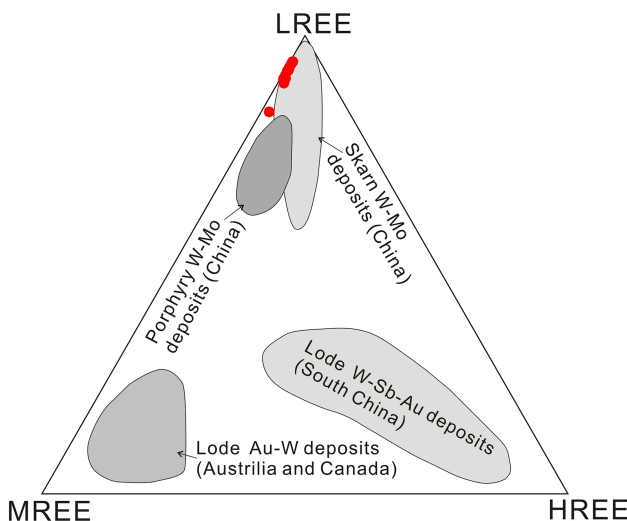


Fig. 8 Triangular LREE–MREE–HREE diagram of the scheelite from the Kukaazi deposit (areas for scheelite samples from other kinds of deposits were copied from Song et al. 2014)

Bulong granite (441 Ma, Wang et al. 2013a). Therefore, the activity of these granitic magmas could last at least ca. 30 million years in the Kukaazi deposit and adjacent areas, covering the timing of W–Mo mineralization.

As stated above, in spite of a large area of the Early Paleozoic (from the Cambrian to Silurian) granitoids exposed in the western Kunlun area, there are no metallic ore deposits reported to be associated with the Early Paleozoic granite intrusions yet. In this study, we provided confident isotopic ages to prove that the Early Paleozoic granitoids (i.e. Ordovician) could lead to economic Mo–W–(Cu) mineralization at favorable districts in the western Kunlun. This result would extend our understanding on the

regional metallogenesis, and be greatly helpful for the prospecting explorations in this region.

6.2 Source of ore-forming materials

As a kind of Ca-rich minerals in many hydrothermal deposits, scheelite is rich in some trace elements, including REE and Sr, which can substitute Ca^{2+} in the crystal lattice of scheelite in form of isomorphic replacement (Bell et al. 1989; Voicu et al. 2000; Brugger et al. 2002). Chemistry of scheelite is thus commonly used to trace the source of ore-forming fluids (e.g., Frei et al. 1998; Peng et al. 2003, 2006).

REE contents of scheelite are affected or controlled by compositions of the hydrothermal fluids and wall rocks (Peng et al. 2005). In this study, REE patterns (especially the LREE part) of the scheelite are similar to those of the coeval granitoids in the region (Fig. 7), suggesting that the scheelite could be precipitation from the magmatic-hydrothermal fluids that were exsolved from such granitoids in the region. However, the scheelite from the Kukaazi deposit has relatively lower REE contents (especially for HREE and Y) than the granitoid (Fig. 7), which could be attributed to the early precipitation of skarn minerals (e.g., garnet and diopside) that extracted most of HREEs from ore-forming fluids (Song et al. 2014).

Since Eu can substitute Ca^{2+} (ionic radius 1.06 Å) in scheelite as a state of either Eu^{3+} (0.947 Å) or Eu^{2+} (1.17 Å), the Eu anomalies in scheelite could be ascribed to the redox conditions of ore-forming fluids (Ghaderi et al. 1999; Brugger et al. 2000, 2002, 2008). Previous studies have demonstrated that a high concentration of Eu^{2+} ($\text{Eu}^{3+} < \text{Eu}^{2+}$) in reduced fluids would result in a positive Eu anomaly in scheelite, while oxidized fluids would have higher proportion of Eu^{3+} ($\text{Eu}^{3+} > \text{Eu}^{2+}$), leading to a negative Eu anomaly in precipitated minerals (Ghaderi et al. 1999; Xiong et al. 2006). All analyzed scheelite from the Kukaazi deposit has strongly negative Eu anomalies with δEu values of 0.13–0.55, indicative of oxidized ore-forming fluids. The oxidized nature of ore-forming fluids also supports the linkage with I-type granitic magmatism.

Neodymium is one of the light REE so that its isotopic compositions of the geological body bear information of the original source of the REE. The $\varepsilon_{\text{Nd}}(t)$ value of scheelite can be used to trace the source of the ore-forming fluid precipitating scheelite (Peng et al. 2008). On the other hand, scheelite is a Ca-bearing mineral that can limit the accommodation of Rb in Ca ion positions of its crystal lattice (Deer et al. 1992), resulting in extremely low Rb/Sr ratios in scheelite. As such, the radioactive ^{87}Sr from the decay of ^{87}Rb after its formation is negligible. Moreover, Sr isotopic fractionation during mineral precipitation in the hydrothermal system is less than 0.2‰ (Krabbenhoef et al.

2010), much lower than the radiogenic variation of $^{87}\text{Sr}/^{86}\text{Sr}$ in natural hydrothermal systems. Therefore, the measured $^{87}\text{Sr}/^{86}\text{Sr}$ ratios of the scheelite can approximately reflect the initial Sr isotopic compositions of the fluids where the mineral precipitated. The scheelite from the Kukaazi deposit has uniform low $\epsilon_{\text{Nd}}(\text{t})$ values, with the T_{DM} values of 1.5–1.2 Ga. Meanwhile, the scheelite exhibits relatively highly radiogenic $^{87}\text{Sr}/^{86}\text{Sr}$ ratios of 0.7107–0.7118. These isotopic data broadly agree with those of the coeval granitoids in the region (Yuan et al. 2003; Jia 2013). The Sr–Nd isotopes further suggest that the W-mineralizing fluids of the Kukaazi deposit could be derived from the granitoids.

7 Conclusions

1. The Mo and W mineralization at the Kukaazi deposit formed at ca. 450 Ma, and was closely related to the intrusion of the Ordovician granitoid in the deposit.
2. The scheelite displays similar REE patterns, Sm/Nd ratios and Sr and Nd isotopic compositions to those of the coeval granitoids in the mine, suggesting that the tungsten probably originates from such granitoids.
3. We identified the Ordovician granitoids could lead to economic Mo–W–(Cu) mineralization at some favorable districts in the western Kunlun area. This extends our understanding of the regional metallogenesis and is helpful for the prospecting explorations in this region.

Acknowledgements This work is funded by a “Chinese NSF” Project (41272114) to Xingchun Zhang, a “CAS Western Light Talent Culture” Project to Chengbiao Leng, and a “CAS Hundred Talents” Project to Jianfeng Gao. Jin Hu is specially thanked for her kind help in REE analysis. We highly appreciate Wei Terry Chen for his helpful suggestions and language improvement on drafts of this manuscript.

References

- Bell K, Anglin C, Franklin J (1989) Sm–Nd and Rb–Sr isotope systematics of scheelites: possible implications for the age and genesis of vein-hosted gold deposits. *Geology* 17:500–504
- Boynton WV (1984) Geochemistry of the rare earth elements: meteorite studies. In: Henderson P (ed) Rare Earth Element Geochemistry. Elsevier, Amsterdam, pp 63–114
- Brugger J, Lahaye Y, Costa S, Lambert D, Bateman R (2000) Inhomogeneous distribution of REE in scheelite and dynamics of Archaean hydrothermal systems (Mt. Charlotte and Drysdale gold deposits, Western Australia). *Contrib Miner Petrol* 139:251–264
- Brugger J, Maas R, Lahaye Y, McRae C, Ghaderi M, Costa S, Lambert D, Bateman R, Prince K (2002) Origins of Nd–Sr–Pb isotopic variations in single scheelite grains from Archaean gold deposits, Western Australia. *Chem Geol* 182:203–225
- Brugger J, Etschmann B, Pownceby M, Liu WH, Grundler P, Brewe D (2008) Oxidation state of europium in scheelite: tracking fluid–rock interaction in gold deposits. *Chem Geol* 257:26–33
- Chesley J, Halliday A, Scrivener R (1991) Samarium–neodymium direct dating of fluorite mineralization. *Science* 252:949–951
- Cui JT, Wang JC, Bian XW, Zhu HP, Yang KJ (2006) Geological characteristics of Early Paleozoic amphibolite and tonalite in northern Kangxiwar, West Kunlun, China and their zircon SHRIMP U–Pb dating. *Geol Bull China* 25:1441–1449 (in Chinese with English abstract)
- Cui JT, Wang JC, Bian XW, Zhu HP, Luo QZ, Yang KJ, Wang MC (2007) Zircon SHRIMP U–Pb dating of Early Paleozoic granite in the Menggubao–Pushou area on the northern side of Kangxiwar, West Kunlun. *Geol Bull China* 26:710–719 (in Chinese with English abstract)
- Deer W, Howie R, Zussman J (1992) An introduction to the rock-forming minerals. Longman Sci Tech 66:509–517
- Du AD, He HY, Yin WN, Zhou XQ, Sun YL, Sun DZ, Chen SZ, Qu WJ (1994) The study on the analytical methods of Re–Os age for molybdenites. *Acta Geol Sin* 68:339–347 (in Chinese with English abstract)
- Du AD, Wu SQ, Sun DZ, Wang SX, Qu WQ, Markey R, Stain H, Morgan J, Malinovskiy D (2004) Preparation and Certification of Re/Os Dating Reference Materials: molybdenites HLP and JDC. *Geostand Geanal Res* 28:41–52
- Fang XL, Wang YZ (1990) Preliminary discussion on caledonian granites in western kunlun mountains. *Xinjiang Geol* 8:153–158 (in Chinese with English abstract)
- Frei R, Nagler TF, Schonberg R, Kramers JD (1998) Re–Os, Sm–Nd, U–Pb, and stepwise lead leaching isotope systematics in shear-zone hosted gold mineralization: genetic tracing and age constraints of crustal hydrothermal activity. *Geochim Cosmochim Acta* 62:1925–1936
- Ghaderi M, Palin JM, Campbell IH, Sylvester PJ (1999) Rare earth element systematics in scheelite from hydrothermal gold deposits in the Kalgoorlie–Norseman region, Western Australia. *Econ Geol* 94:423–437
- Jia RY (2013) Petrogenesis and tectonic implications of Qiukesugranite pluton and its enclaves in the western Kunlun Orogen Belt, NW China. Dissertation for master’s degree of Nanjing Universit, 1–62
- Jiang YH, Rui XJ, He JR, Guo KY, Yang WZ (1999) Tectonic type of Caledonian granitoids and tectonic significance in the West Kunlun Mts. *Acta Petrol Sin* 15:105–115 (in Chinese with English abstract)
- Jiang YH, Rui XJ, Guo KY, He JR (2000) Tectonic environments of granitoids in the West Kunlun orogenic blet. *Acta Geosci Sin* 21:23–25 (in Chinese with English abstract)
- Krabbenhoft A, Eisenhauer A, Boehm F, Vollstaedt H, Fietzke J, Liebetrau V, Augustin N, Peucker-Ehrenbrink B, Mueller MN, Horn C, Hansen BT, Nolte N, Wallmann K (2010) Constraining the marine strontium budget with natural strontium isotope fractionations ($^{87}\text{Sr}/^{86}\text{Sr}^*$, $^{88}\text{Sr}/^{86}\text{Sr}$) of carbonates, hydrothermal solutions and river waters. *Geochim Cosmochim Acta* 74:4097–4109
- Liu Y, Deng J, Li C, Shi G, Zheng A (2007) REE composition in scheelite and scheelite Sm–Nd dating for the Xuebaoding W–Sn–Be deposit in Sichuan. *Chin Sci Bull* 52:2543–2550
- Liu JP, Wang H, Li SH, Tong LX, Ren GL (2010) Geological and geochemical features and geochronology of the Kayizi porphyry molybdenum deposit in the northern belt of western Kunlun, NW China. *Acta Petrol Sin* 26:3095–3105 (in Chinese with English abstract)
- Liu Y, Zhang RQ, Abuduwayiti M, Wang C, Zhang S, Shen C, Zhang Z, He M, Zhang Y, Yang X (2016) SHRIMP U–Pb zircon ages, mineral compositions and geochemistry of placer nephrite in the Yurungkash and Karakash River deposits, West Kunlun, Xinjiang, northwest China: implication for a Magnesium Skarn. *Ore Geol Rev* 72:699–727

- Ludwig K (2012) User's manual for Isoplot version 3.75–4.15: a geochronological toolkit for Microsoft Excel. Berkley Geochronological Center special publication no. 5
- Mattern F, Schneider W (2000) Suturing of the proto- and paleo-tethys oceans in the western Kunlun (Xinjiang, China). *J Asian Earth Sci* 18:637–650
- Mattern F, Schneider W, Li Y, Li X (1996) A traverse through the western Kunlun (Xinjiang, China): tentative geodynamic implications for the Paleozoic and Mesozoic. *Geol Rundsch* 85:705–722
- Pan YS (1989) A preliminary study on the regionalization of the structures in the Kunlun mountains region. *J Nat Resour* 4:196–203 (in Chinese with English abstract)
- Pan YS, Wang Y, Matte P, Tappognier P (1994) Tectonic evolution along the geotraverse from Yecheng to Shiquanhe. *Acta Geosci Sin* 68:295–307 (in Chinese with English abstract)
- Peng JT, Hu RZ, Zhao JH, Fu YZ, Lin YX (2003) Scheelite Sm–Nd dating and quartz Ar–Ar dating for Woxi Au–Sb–W deposit, western Hunan. *Chin Sci Bull* 48:2640–2646
- Peng JT, Hu RZ, Zhao JH, Fu YZ, Yuan SD (2005) Rare earth element (REE) geochemistry for scheelite from the Woxi Au–Sb–W deposit, western Hunan. *Geochimica* 34:115–122 (in Chinese with English abstract)
- Peng B, Frei R, Tu XL (2006) Nd–Sr–Pb Isotopic Geochemistry of Scheelite from the Woxi W–Sb–Au Deposit, Western Hunan Implications for Sources and Evolution of Ore-forming Fluids. *Acta Geosci Sin* 80:561–570 (in Chinese with English abstract)
- Peng JT, Zhang DL, Hu RZ, Wu MJ, Lin YX (2008) Sm–Nd and Sr Isotope Geochemistry of Hydrothermal Scheelite from the Zhazixi W–Sb Deposit, Western Hunan. *Acta Geosci Sin* 82:1514–1521 (in Chinese with English abstract)
- Qi L, Hu J, Gregoire DC (2000) Determination of trace elements in granites by inductively coupled plasma mass spectrometry. *Talanta* 51:507–513
- Robb L (2005) Introduction to ore-forming processes. Blackwell Publishing House, London, p 373
- Smoliar MI, Walker RJ, Morgan JW (1996) Re–Os ages of group IIA, IIIA, IVA, and IVB iron meteorites. *Science* 271:1099–1102
- Song GX, Qin KZ, Li GM, Evans NJ, Chen L (2014) Scheelite elemental and isotopic signatures: implications for the genesis of skarn-type W–Mo deposits in the Chizhou Area, Anhui Province, Eastern China. *Am Miner* 99:303–317
- Stein HJ, Markey RJ, Morgan JW, Du A, Sun Y (1997) Highly precise and accurate Re–Os ages for molybdenite from the East Qinling molybdenum belt, Shaanxi Province, China. *Econ Geol* 92:827–835
- Sun HT, Li CJ, Wu H, Wang HJ, Qi SJ, Chen GM, Liu ZT, Gao P (2003) Introduction to the West KunLun metallogenic province. Geological Publishing House, Beijing (in Chinese)
- Voicu G, Bardoux M, Stevenson R, Jebrak M (2000) Nd and Sr isotope study of hydrothermal scheelite and host rocks at Omai, Guiana Shield: implications for ore fluid source and flow path during the formation of orogenic gold deposits. *Miner Depos* 35:302–314
- Wang C, Liu L, Che ZC, He SP, Li RS, Yang WQ, Cao YT, Zhu XH (2009) Zircon U–Pb and Hf isotopic from the east segment of Tiekelike tectonic belt: constrains on the timing of Precambrian basement at the southwestern margin of Tarim, China. *Acta Geosci Sin* 83:1647–1656 (in Chinese with English abstract)
- Wang C, Liu L, He SP, Yang WQ, Cao YT, Zhu XH, Li RS (2013a) Early Paleozoic magmatism in west Kunlun: constraints from geochemical and zircon U–Pb–Hf isotopic studies of the Bulong granite. *Chin J Geol* 48:997–1014 (in Chinese with English abstract)
- Wang YH, Len CB, Zhang XC (2013b) A-preliminary study on elemental geochemistry and geochronology of intermediate-acidic intrusive rocks from Kukaazi Pb–Zn–Cu–W polymetallic deposit, Yecheng County, Xinjiang. *Bull Mineral Petrol Geochem* 32:736–745 (in Chinese with English abstract)
- Xiao WJ, Windley BF, Chen HL, Zhang GC, Li JL (2002) Carboniferous-Triassic subduction and accretion in the western Kunlun, China: implications for the collisional and accretionary tectonics of the northern Tibetan Plateau. *Geology* 30:295–298
- Xiao XC, Wang J, Sun L, Song SG (2003) A further discussion of the Kudi ophiolite, west Kunlun, and its tectonic significance. *Geol Bull China* 22:745–750 (in Chinese with English abstract)
- Xiao WJ, Windley BF, Liu DY, Jian P, Liu CZ, Yuan C, Sun M (2005) Accretionary tectonics of the Western Kunlun Orogen, China: a Paleozoic-Early Mesozoic, long-lived active continental margin with implications for the growth of southern Eurasia. *J Geol* 113:687–705
- Xiong DX, Sun XM, Shi GY, Wang SW, Gao JF, Xue T (2006) Trace elements, rare earth elements (REE) and Nd-Sr isotopic compositions in scheelites and their implications for the mineralization in Daping gold mine in Yunnan Province, China. *Acta Petrol Sin* 22:733–741 (in Chinese with English abstract)
- Xu RH, Zhang YQ, Xie YW, Chen FK, Arnaud N (1994) A-discovery of an Early Paleozoic Tectono-magmatic Belt in the northern part of west Kunlun Mountains. *Sci Geol Sin* 29:313–328 (in Chinese with English abstract)
- Xu ZQ, Yang JS, Li HB, Ji SC, Zhang ZM, Liu Y (2011) On the tectonics of the India-Asia collision. *Acta Geosci Sin* 85:1–33 (in Chinese with English abstract)
- Xu ZQ, Dilek Y, Cao H, Robinson P, Ma CQ, Li HQ, Jolivet M, Roger F, Chen XJ (2015) Paleo-Tethyan evolution of Tibet as recorded in the east Cimmerides and west Cathaysides. *J Asian Earth Sci* 105:320–337
- Yin A, Harrison TM (2000) Geologic evolution of the Himalayan–Tibetan orogen. *Annu Rev Earth Plan Sci* 28:211–280
- Yu XF, Sun FM, Li BL, Ding QF, Chen GJ, Ding ZJ, Chen J, Huo L (2011) Caledonian diagenetic and metallogenetic events in Datong District in the western Kunlun: evidence from LA-ICP-MS zircon U–Pb dating and molybdenite Re–Os dating. *Acta Petrol Sin* 27:1770–1778 (in Chinese with English abstract)
- Yuan C, Sun M, Zhou MF, Zhou H, Xiao WJ, Li JL (2002) Tectonic evolution of the West Kunlun: geochronologic and geochemical constraints from Kudi Granitoids. *Int Geol Rev* 44:653–669
- Yuan C, Sun M, Xiao WJ, Zhou H, Hou QL, Li JL (2003) Subduction polarity of the prototethys: insights from the Yirba pluton of the western Kunlun range, NW China. *Acta Petrol Sin* 19:399–408 (in Chinese with English abstract)
- Zhang YQ, Xie YW (1989) A study on the Rb–Sr biotite isochron ages of the granitoid in the Sanshiliyifang area of the Karakoram and Kunlun MTS, region. *J Nat Resour* 4:222–227
- Zhang CL, Yu HF, Shen JL, Dong YG, Ye HM, Guo K (2004) Zircon SHRIMP Age Determination of the Giant-crystal Gabbro and Basalt in Kuda, West Kunlun: dismembering of the Kuda Ophiolite. *Geol Rev* 50:639–643 (in Chinese with English abstract)
- Zhang CL, Yu HF, Wang AG, Guo KY (2005) Dating of Triassic granites in the Western Kunlun mountains and its tectonic significance. *Acta Geosci Sin* 79:645–652 (in Chinese with English abstract)
- Zhang CL, Lu SN, Yu HF, Ye H (2007) Tectonic evolution of the Western Kunlun orogenic belt in northern Qinghai-Tibet Plateau: evidence from zircon SHRIMP and LA-ICP-MS U–Pb geochronology. *Sci China Ser D Earth Sci* 50:825–835
- Zhang CL, Zou HB, Santosh M, Ye XT, Li HK (2014a) Is Precambrian basement of the Tarim Craton in NW China composed of discrete terranes? *Precambrian Res* 254:226–244

- Zhang XC, Wang YH, Leng CB, Zhang W, Xu LL, Zhu JJ, Chen YW (2014b) Geology, sulfur isotopes and scheelite Sm–Nd age of the Kukazzi Pb–Zn–(Cu–W) polymetallic deposit, Yecheng County, Xinjiang, China. *Acta Geol Sin Engl* 88:244–246
- Zhang ZW, Shen NP, Peng JT, Yang XR, Feng GY, Yu F, Zhou LJ, Li YJ, Wu CQ (2014c) Syndeposition and epigenetic modification of the strata-bound Pb–Zn–Cu deposits associated with carbonate rocks in western Kunlun, Xinjiang, China. *Ore Geol Rev* 62:227–244
- Zhang Y, Niu YL, Hu Y, Liu JJ, Ye L, Kong JJ, Duan M (2015) The syncollisional granitoid magmatism and continental crust growth in the West Kunlun Orogen, China—evidence from geochronology and geochemistry of the Arkarz pluton. *Lithos* 245:191–204